

These observations indicate that there is an additional nonradiative decay mechanism for **1** in solvents of relatively low polarity which may be the charge transfer facilitated by the termolecular interaction.<sup>19</sup>

Equally significant in our observations is the emission characteristics of **1c**. The solvent dependence plot on the emission maximum is a nonlinear one (Figure 1).<sup>23</sup> Although the position of fluorescence maximum of **1c** is indistinguishable from those of **1a** and **2a** in nonpolar solvents, they began to deviate substantially in solvents more polar than ether. If we divide the plot into portions, one including solvents from pentane to ether and the other including *n*-butyl acetate to dichloromethane, the results may be fitted into two lines of slopes of  $(-5.30 \pm 0.60) \times 10^3$  and  $(-15.5 \pm 1.3) \times 10^3 \text{ cm}^{-1}$ , respectively.<sup>24</sup> The data indicate that **1c** will form a binary intramolecular exciplex similar to **1a** or **2a** in nonpolar solvents, while in a more polar solvent it will form a ternary exciplex similar to that of **1b**. In spite of the difference in the IP of the dimethyl derivatives of *p*-anisidine and *p*-toluidine,<sup>25</sup> model compounds for the second nitrogen in **1b** and **1c**, the apparent dipole moments of exciplex derived from **1c** in solvents more polar than ether is very similar to those from **1b**. This result further substantiates the existence of intramolecular ternary exciplex **4**. Our results also imply that in a solvent of intermediate polarity such as ether both emitting species from **1c** may coexist in solution. Since exciplex emissions are broad and structureless in nature, two close-by emissions from **1c** are not resolvable from its emission spectra. In order to gain further insight into this problem, we determined the lifetimes of these exciplexes by kinetic spectroscopy, and the results are tabulated in the table. While all other exciplexes from these compounds exhibit single exponential decay, **1c** in ether exhibits a decay that is best fitted by a double-exponential function. This observation supports the existence of two emitting species from **1c** in ether.

On the basis of above observations, we conclude that (a) under proper experimental conditions, trichromophoric **1** may exist as an intramolecular ternary exciplex **4**, (b) **4** is stabilized relative to the binary exciplex **3** by increasing the polarity of the solvent, and (c) **4**, being more polar than **3**, undergoes nonradiative decay more efficiently than **3** in relatively nonpolar solvents, most likely due to ion-pair formation.

**Acknowledgment.** We thank the National Science Foundation, Grants No. CHE-81-12964 and CHE-80-09216, for the support of this work and Professor Graham Fleming for his advice, assistance, and encouragement.

**Registry No.** **1a**, 82665-24-5; **1b**, 82665-25-6; **1c**, 82665-26-7; **2a**, 55789-86-1; **2b**, 55789-88-3; I, 41034-83-7; II, 22689-05-0; III, 82665-27-8; IV, 82665-28-9; V, 82665-29-0; VI, 82665-30-3; acrylic acid, 79-10-7; *N*-methyl-aniline, 100-61-8; *N,N,N',N'*-tetramethyl-*p*-phenylenediamine, 100-22-1; *N,N,N',N'*-tetramethyl-*p*-phenylenediamine 1,3,5-trinitrobenzene, 41912-16-7; *N,N,N',N'*-tetramethyl-*p*-phenylenediamine chloranil, 27237-38-3; *N,N,N',N'*-tetramethyl-*m*-phenylenediamine, 22440-93-3; *N,N,N',N'*-tetramethyl-*m*-phenylenediamine 1,3,5-trinitrobenzene, 82665-31-4; *N,N,N',N'*-tetramethyl-*m*-phenylenediamine chloranil, 82665-35-8; *N,N*-dimethyl-3,4-xylylidene, 770-03-6; *N,N*-dimethyl-3,4-xylylidene 1,3,5-trinitrobenzene, 82665-32-5; *N,N*-dimethyl-3,4-xylylidene chloranil, 82665-36-9; *N,N*-dimethyl-*p*-anisidine, 701-56-4; *N,N*-dimethyl-*p*-anisidine 1,3,5-trinitrobenzene, 82665-33-6; *N,N*-dimethyl-*p*-anisidine chloranil, 82665-37-0; *N,N*-dimethyl-*p*-toluidine, 99-97-8; *N,N*-dimethyl-*p*-toluidine 1,3,5-trinitrobenzene, 82665-34-7; *N,N*-dimethyl-*p*-toluidine chloranil, 20755-56-0; *N,N*-dimethylaniline, 121-

69-7; *N,N*-dimethylaniline 1,3,5-trinitrobenzene, 16636-09-2; *N,N*-dimethylaniline chloranil, 82665-30-3.

**Supplementary Material Available:** Method of preparation, spectral data, and analytical results for compounds **1a-c** and the EDA complex method used to determine the ionization potentials of dimethylaniline, *N,N*-dimethyl-*p*-toluidine, and *N,N*-dimethyl-*p*-anisidine (6 pages). Ordering information is given on any current masthead page.

## Measurement of Spin-Spin Distances from the Intensity of the EPR Half-Field Transition

Sandra S. Eaton

Department of Chemistry, University of Colorado at Denver  
Denver, Colorado 80202

Gareth R. Eaton\*

Department of Chemistry, University of Denver  
Denver, Colorado 80208  
Received May 3, 1982

In systems containing two paramagnetic centers there is frequently considerable interest in determining the distance between the two electron spins.<sup>1</sup> The separation  $2D$  between the low-field and high-field turning points in glass or powder EPR spectra has generally been used to obtain  $r$ , the interspin distance.<sup>2</sup> This analysis of the spectra is only valid under certain conditions. It assumes that the interaction between the two spins is purely dipolar or that the exchange interaction between the spins is sufficiently large that only transitions between triplet levels are observed (Figure 1, transitions 2 and 3). For intermediate values of the exchange coupling constant  $J$ , the observed separation between the turning points in the rigid spectrum is a sum of exchange and dipolar contributions. If the exchange component is ignored, the interspin distance will be underestimated or overestimated, depending on the sign of  $J$ . Even if the magnitude of the exchange interaction permits analysis of the spectra in terms of a purely dipolar interaction, the choice of the turning points that correspond to a separation of  $2D$  may be complicated by large nuclear hyperfine coupling. If the interspin vector  $\vec{r}$  does not coincide with a principal axis of the hyperfine tensor for both of the electrons, then the turning points in the powder spectra will depend on the relative orientations of the hyperfine tensors and dipole tensor and on the relative magnitudes of the hyperfine and dipolar interactions. Without a computer simulation  $2D$  cannot be obtained from these spectra. Also, when the EPR spectra are poorly resolved, it is difficult to estimate  $2D$ . Therefore it would be desirable to have another method to estimate the interspin distance.

We have done a perturbation calculation for two nonequivalent unpaired electrons. Nuclear hyperfine coupling was included for both electrons, and the angles between the nuclear hyperfine tensors and the interspin vector were allowed to take any values. The spin-spin interaction component of the Hamiltonian is given in eq 1, where  $\vec{\mu}_1$  and  $\vec{\mu}_2$  are the magnetic moments for spins 1

$$\mathcal{H}_{\text{int}} = \frac{\vec{\mu}_1 \cdot \vec{\mu}_2}{r^3} - \frac{3(\vec{\mu}_1 \cdot \vec{r})(\vec{\mu}_2 \cdot \vec{r})}{r^5} - J\vec{S}_1 \cdot \vec{S}_2 \quad (1)$$

and 2,  $\vec{r}$  is the interspin vector, and  $J$  is the isotropic exchange constant. The treatment of the nonequivalent spins is similar to that used by Pilbrow and co-workers to analyze the EPR of a  $B_{12}$ -dependent enzyme: substrate system.<sup>3,4</sup> It is assumed that symmetric anisotropic exchange can be neglected. Previous

(23) Nonlinear  $\nu_{\text{ex}}$  vs.  $f - 1/2f'$  plots for **1c** were obtained in two mixed-solvent systems, hexane-dichloromethane and methylcyclohexane-tetrahydrofuran, which are within experimental error of the one recorded in the figure. The corresponding plots for both **1a** and **2a** were found to be linear.

(24) If one includes only the points obtained in solvents ranging from pentane to ether for **1a** and **2a**, the slopes of  $\nu_{\text{ex}}$  vs.  $f - 1/2f'$  plots of these compounds are also  $\approx -5 \times 10^3 \text{ cm}^{-1}$ .

(25) The IP's of *N,N*-dimethyl-*p*-toluidine and *N,N*-dimethyl-*p*-anisidine were determined by the EDA complex method using either 1,3,5-trinitrobenzene or chloranil as the acceptor. The  $\lambda_{\text{max}}$  of the anisidine complexes are 8 nm to the red of that of the toluidine complexes. The IP's of dimethylaniline, *N,N*-dimethyl-*p*-toluidine, and *N,N*-dimethyl-*p*-anisidine are estimated to be 7.13, 7.07, and 7.03 eV, respectively.

(1) Eaton, G. R.; Eaton, S. S. *Coord. Chem. Rev.* **1978**, *26*, 207-262.

(2) Luckhurst, G. R. In "Spin Labeling: Theory and Applications", Berliner, L. J., Ed.; Academic Press: New York, 1976; Chapter 4, particularly Figure 4 and eq 49.

(3) Boas, J. F.; Hicks, P. R.; Pilbrow, J. R. *J. Chem. Soc., Faraday Trans.* **1978**, *74*, 417-431.

(4) Eaton, S. S.; Eaton, G. R., to be submitted for publication.

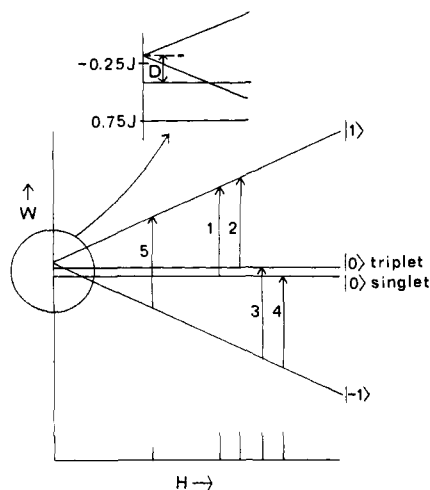


**Figure 1.** Energy level diagram for two interacting spins showing the effect of isotropic exchange and dipolar interaction when the magnetic field is along the  $z$ -axis of the dipolar tensor. The Hamiltonian for the interaction is given by eq 1. This diagram is drawn for  $J < 0$ . The dipolar interaction within the triplet state causes the separation  $D$  between the  $|0\rangle$  and  $|\pm 1\rangle$  states as shown in the insert. The  $\Delta M_s = \pm 1$  transitions are labeled 1–4 and the  $\Delta M_s = \pm 2$  transition is labeled 5.

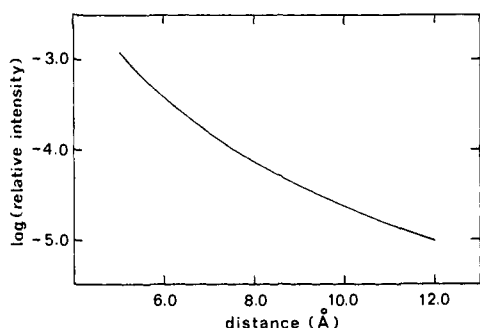
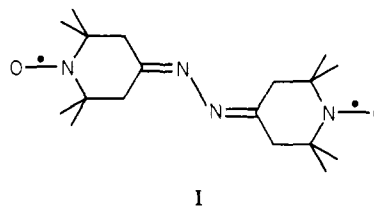


**Figure 2.** Dependence of the intensity of the half-field transition on the interspin distance,  $r$ , in Å. Relative intensity is defined as (intensity of transition 5)/(total intensity of transitions 1–4), where the transitions are defined as in Figure 1.

discussions of the determination of the interspin distance have focused on the  $\Delta M_s = \pm 1$  transitions (Figure 1, transitions 1–4). In this communication we emphasize the utility of the half-field or  $\Delta M_s = \pm 2$  transition (Figure 1, transition 5) in analyzing dipolar interactions. To first approximation, exchange causes mixing of the singlet and triplet  $M_s = 0$  levels and does not effect the triplet  $M_s = \pm 1$  levels. Dipolar interaction shifts the energies of the  $M_s = \pm 1$  levels to the same extent. Thus the energy of the  $\Delta M_s = \pm 2$  transition is essentially independent of the magnitudes of  $J$  and  $\bar{r}$ . The intensity of the half-field transition is greatest when the angle between the magnetic field and the interspin vector (the  $z$  axis for the dipolar interaction), is about  $45^\circ$ , so the line

shape of the half-field signal is largely determined by the nuclear hyperfine couplings at these orientations. Therefore the line shape is a sensitive monitor of the relative orientations of the spin–spin vector and the nuclear hyperfine axes. Unlike the line shape, the integrated intensity of the half-field transition is determined by the strength of the dipolar interaction and varies as  $r^{-6}$ , which makes it a sensitive indicator of the magnitude of  $\bar{r}$ . We have chosen to express the intensity as the ratio of the intensity of transition 5 to the combined intensity of transitions 1–4. The use of the ratio of intensities for two portions of the spectra for the same sample eliminates the need for many of the correction factors that would otherwise be required for accurate intensity determination.<sup>5,6</sup> Figure 2 shows the log of the intensity ratio as a function of  $r$  calculated for two spins with  $g \sim 2$ . The calculated dependence of intensity on  $r$  is given by: relative intensity  $\approx 20/r^6$ . The values are insensitive to the magnitude of  $J$ , provided  $J$  is small relative to  $kT$ . Since the dipolar interaction depends on the electron  $g$  values, a different curve would be obtained for systems with  $g$  values not equal to 2.

To calibrate the accuracy of the calculated curve, we examined the half-field transitions for several compounds with well-defined structures. Three spin-labeled copper complexes were studied. CPK molecular models indicated copper–nitroxyl distances of 5–6.5 Å. When the relative intensities of the half-field transitions were compared with the graph in Figure 2, the calculated distances agreed with the distances obtained from the models within 0.5 Å. Single-crystal EPR studies of dinitroxyl I indicated a spin–spin



distance of 8.2 Å.<sup>7</sup> On the basis of the relative intensity of the half-field transition we obtained 8.5 Å. Further calibration checks are underway for other molecules with relatively rigid geometries and known structures. Based on the data obtained to date, it appears that the calculations agree well with the experimental data.

The intensity of the half-field transition should serve as a powerful tool for the determination of spin–spin distances. Its use is subject to fewer restrictions than the use of the splitting  $2D$ . The curve in Figure 2 is appropriate only for  $S = 1/2$  ions with  $g \sim 2$  at X bond, but comparable curves can be obtained for other ions and frequencies.

**Acknowledgment.** This work was supported in part by NIH Grant GM 21156.

(5) Eaton, G. R.; Eaton, S. S. *Bull. Magn. Reson.* **1980**, *1*, 130–138.

(6) Goldberg, I. B. *Electron Spin Reson.* **1981**, *6*, 1–23.

(7) Nakajima, A. *Bull. Chem. Soc. Jpn.* **1973**, *46*, 1129–1134.